Research Article

Numerical Investigation on Convergence Rate of Singular Boundary Method

Junpu Li, Wen Chen, and Zhuojia Fu

State Key Laboratory of Hydrology-Water Resources and Hydraulic Engineering, Center for Numerical Simulation Software in Engineering and Sciences, College of Mechanics and Materials, Hohai University, Nanjing 210098, China

Correspondence should be addressed to Wen Chen; chenwen@hhu.edu.cn

The singular boundary method (SBM) is a recent boundary-type collocation scheme with the merits of being free of mesh and integration, mathematically simple, and easy-to-program. Its essential technique is to introduce the concept of the source intensity factors to eliminate the singularities of fundamental solutions upon the coincidence of source and collocation points in a strong-form formulation. In recent years, several numerical and semianalytical techniques have been proposed to determine source intensity factors. With the help of these latest techniques, this short communication makes an extensive investigation on numerical efficiency and convergence rates of the SBM to an extensive variety of benchmark problems in comparison with the BEM. We find that in most cases the SBM and BEM have similar convergence rates, while the SBM has slightly better accuracy than the direct BEM. And the condition number of SBM is lower than BEM. Without mesh and numerical integration, the SBM is computationally more efficient than the BEM.

1. Introduction

The boundary element method (BEM) [1–4] and the method of fundamental solutions (MFS) [5–8] are two important numerical methods for science and engineering applications. However, it is a sophisticated mathematical and time-consuming issue for numerical integration over the singularities in the BEM. As for the MFS, the location of fictitious boundary is vital for its numerical accuracy and reliability and remains an open issue to optimally determine especially for complex-shaped or multiconnected domain problems.

To remedy these drawbacks in the BEM and MFS, several numerical schemes have been proposed, such as the boundary collocation method (BCM) [9], the modified collocation Trefftz method (MCTM) [10–12], the regularized meshless method (RMM) [13–16], the modified method of fundamental solutions (MMFS) [17], the boundary distributed source (BDS) method [18–20], and the nonsingular method of fundamental solutions [21].

The singular boundary method (SBM) [22] was proposed by the authors in 2009 and is a strong-form boundary discretization technique. In order to regularize the singularities of fundamental solutions upon the coincidence of source and collocation points, the concept of the source intensity factors (SIFs) was first introduced, which is also called the origin intensity factors (OIFs) in some literatures [22]. Under the extensive studies, four techniques have been proposed to determine the source intensity factors of both the fundamental solution and its derivative, namely, inverse interpolation technique (IIT), semianalytical technique with subtracting and adding-back desingularization (SAT1), semianalytical technique with integral mean value approach (SAT2), and semianalytical technique with the empirical formula (SAT3). Numerical investigation shows that the SBM can provide accurate solutions in potential [22], Helmholtz [23], acoustic and elastic waves [24, 25], and water wave problems [26] with arbitrarily complex-shaped computational geometries.

This short communication will make a comparison on numerical efficiency and convergence rate under the extensive benchmark testing with the best approach to determining the source intensity factors. A brief outline of the paper is as follows: Section 2 will describe the techniques to determine SIFs which will be used in Section 3 for solving 2D and 3D Laplace, Helmholtz, and modified Helmholtz equations.

Section 3 will make a comparison on numerical efficiency and convergence rate under the extensive benchmark testing in comparison with the direct BEM. At last, Section 4 will make a conclusion.

2. The Latest Techniques to Determine Source Intensity Factors

This section will describe the techniques to determine source intensity factors for solving 2D and 3D Laplace, Helmholtz, and modified Helmholtz equations.

2.1. SBM for Laplace Equations. This section describes the SBM for Laplace equations. Consider the Laplace equations:

$$\Delta u(x) = 0, \quad x \in \Omega,$$
$$u(x) = \overline{u}(x), \quad x \in \Gamma_D,$$
$$\frac{\partial u(x)}{\partial \mathbf{n}} = \frac{\partial \overline{u}(x)}{\partial \mathbf{n}}, \quad x \in \Gamma_N, \tag{1}$$

where Δ denotes the Laplacian operator, the solutions $u(x)$ are the potentials in domain Ω, $\overline{u}(x)$ is the known function, and $\mathbf{n}$ is the unit outward normal on physical boundary. Γ_D and Γ_N represent the essential boundary (Dirichlet) and the natural boundary (Neumann) conditions.

By adopting the fundamental solution G_0 of Laplace equation, the solution $u(x)$ is approximated by a linear combination of fundamental solutions with respect to different source points s_j as below:

$$u(x) = \sum_{j=1}^{N} \alpha_j G_0(x, s_j), \tag{2}$$

where N is the number of source points and α_j is the jth unknown coefficient. The fundamental solution G_0 will have singularities when $x_m = s_j$. To solve this problem, we introduce the concept of source intensity factors in SBM. We place all computing nodes on the same physical boundary. So the source points $\{s_j\}$ and the collocation points $\{x_m\}$ are the same set of boundary nodes. When $x_m = s_j$, we use source intensity factors replacing the singular terms in formulation (2). Thus the SBM formulation can be expressed as

$$u(x_m)$$
$$= \begin{cases} \sum_{j=1}^{N} \alpha_j G_0(x_m, s_j), & x_m \in \Omega \setminus \partial\Omega, \\ \sum_{\substack{j=1 \\ j \neq m}}^{N} \alpha_j G_0(x_m, s_j) + \alpha_m U_0^{jj}, & x_m \in \Gamma_D, \end{cases}$$
$$q(x_m) = \frac{\partial u(x_m)}{\partial \mathbf{n}_x} \tag{3}$$
$$= \begin{cases} \sum_{j=1}^{N} \alpha_j \dfrac{\partial G_0(x_m, s_j)}{\partial \mathbf{n}_x}, & x_m \in \Omega \setminus \partial\Omega, \\ \sum_{\substack{j=1 \\ j \neq m}}^{N} \alpha_j \dfrac{\partial G_0(x_m, s_j)}{\partial \mathbf{n}_x} + \alpha_m Q_0^{jj}, & x_m \in \Gamma_N, \end{cases}$$

where U_0^{jj} and Q_0^{jj} are defined as the source intensity factors corresponding to the fundamental solutions and the unit outward normal of fundamental solutions, namely, the diagonal elements of the SBM interpolation matrix.

Therefore, to solve all kinds of physical and mechanical problems with formulations (3), the key issue is to determine the source intensity factors.

In recent years, four techniques have been proposed to determine the abovementioned source intensity factors. And the merits and demerits of these techniques have already been extensively investigated in some literatures [22–26]. In this study, we only list the best formulations of these techniques to investigate the numerical efficiency and convergence rates of the SBM in comparison with the BEM under several typical benchmark problems.

In this study, we use formulas (4) and (5) to determine the source intensity factors for 2D and 3D Laplace problems with Neumann boundary condition.

The formulation can be expressed as

$$Q_0^{jj} = -V_m - \sum_{\substack{j=1 \\ j \neq m}}^{N} \Pi_j \frac{\partial G_0(x_m, s_j)}{\partial \mathbf{n}_s}, \tag{4}$$

$$U_0^{jj} = \frac{u_I(x_m) - \sum_{j=1, j \neq m}^{N} \alpha_j G_0(x_m, s_j) - \left(u_I(x_I) - \sum_{j=1}^{N} \alpha_j G_0(x_I, s_j)\right)}{\alpha_m}, \tag{5}$$

where x_I is one inner point inside the domain Ω, $u_I = x + y$ is the sample solution in 2D problems, and $u_I = x + y + z$ is the sample solution in 3D problems. G_0 is the fundamental solution of Laplace equation, $\Pi_j = L_j/L_m$, and $\Pi_m = 1$. L_j is the corresponding influence area of source point s_j. For 2D problem, L_j is half length of the curve $s_{j-1}s_{j+1}$ between source points s_{j-1} and s_{j+1} as shown in Figure 1(a). And, for 3D problem, it is the corresponding infinitesimal area as shown in Figure 1(b).

Then, we use the following formula to determine the source intensity factors for 2D Laplace equations with Dirichlet boundary condition:
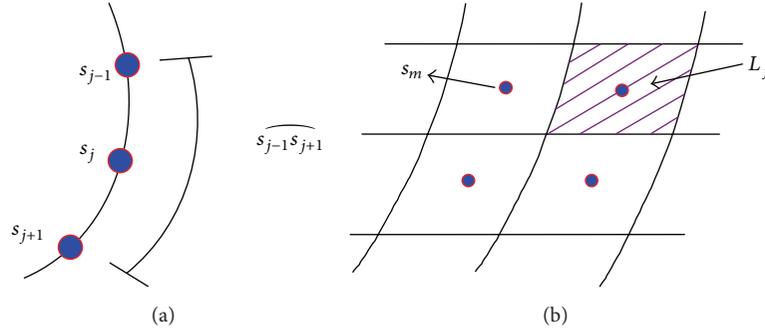
FIGURE 1: The schematic configuration of (a) the source points s_j and the curve $\widehat{s_{j-1}s_{j+1}}$ on 2D problems and (b) the source points s_j and the corresponding infinitesimal area L_j on 3D problems.

$$U_0^{jj} = \frac{\ln\left(L_j/2\pi\right)}{2\pi}. \tag{6}$$

And we use formula (7) to determine the source intensity factors for 3D Laplace equations with Dirichlet boundary condition:

$$U_0^{jj} = \frac{\Theta\left(x_j\right) - \sum_{i=1,i\neq j}^N G_0\left(x_j, s_i\right) L_i}{L_j}, \tag{7}$$

where $\Theta(x_j) = \int_\Gamma G_0(x_j, s)d\Gamma(s)$, $G_0(x_j, s) = 1/4\pi r(x_j, s)$.

Formulas (4) and (5) are also called the semianalytical technique with subtracting and adding-back desingularization (SAT1). Formula (6) is also called the semianalytical technique with the empirical formula (SAT3). Formula (7) is also called the semianalytical technique with integral mean value approach (SAT2). And one can find more details about these techniques in the literatures [22–26].

2.2. SBM for Helmholtz Equations and Modified Helmholtz Equations. In analogy to the SBM for Laplace equations, the corresponding SBM approximate solution for Helmholtz and modified Helmholtz equations can be represented as

$$u\left(x_m\right)$$

$$= \begin{cases} \displaystyle\sum_{j=1}^N \alpha_j G_{ii}\left(x_m, s_j\right), & x_m \in \Omega \setminus \partial\Omega, \\ \displaystyle\sum_{\substack{j=1 \\ j\neq m}}^N \alpha_j G_{ii}\left(x_m, s_j\right) + \alpha_m U^{jj}, & x_m \in \Gamma_D, \end{cases}$$

$$q\left(x_m\right) = \frac{\partial u\left(x_m\right)}{\partial \mathbf{n}_x} \tag{8}$$

$$= \begin{cases} \displaystyle\sum_{j=1}^N \alpha_j \frac{\partial G_{ii}\left(x_m, s_j\right)}{\partial \mathbf{n}_x}, & x_m \in \Omega \setminus \partial\Omega, \\ \displaystyle\sum_{\substack{j=1 \\ j\neq m}}^N \alpha_j \frac{\partial G_{ii}\left(x_m, s_j\right)}{\partial \mathbf{n}_x} + \alpha_m Q^{jj}, & x_m \in \Gamma_N, \end{cases}$$

where U^{jj} and Q^{jj} are the source intensity factors corresponding to the fundamental solution and the unit outward normal of fundamental solution. N is the number of source point. α_j is the jth unknown coefficient, $ii = 1$ or 2. $G_1(x_m, s_j) = (i/4)H_0^{(1)}(kr_{mj})$ is the fundamental solution for 2D Helmholtz equations, $G_2(x_m, s_j) = (1/2\pi)K_0(kr_{mj})$ for 2D modified Helmholtz equations, $G_1(x_m, s_j) = \exp(ikr_{mj})/4\pi r_{mj}$ for 3D Helmholtz problems, and $G_2(x_m, s_j) = \cosh(kr_{mj})/4\pi r_{mj}$ for 3D modified Helmholtz problems. $H_0^{(1)}$ represents the zero-order Hankel function of the first kind, K_0 represents the zero-order modified Bessel function of the second kind, and $r_{mj} = \|x_m - s_j\|_2$ is the Euclidean distance between collocation points x_m and source points s_j.

Due to the property of the same order of the singularities between the fundamental solutions of Helmholtz-type equations and Laplace equation, the source intensity factors of Helmholtz equation and modified Helmholtz equation can be expressed as

$$U^{jj}\left(x_m, s_j\right) = U_0^{jj}\left(x_m, s_j\right) + B, \quad r_{mj} \longrightarrow 0, \tag{9}$$

$$Q^{jj}\left(x_m, s_j\right) = Q_0^{jj}\left(x_m, s_j\right), \quad r_{mj} \longrightarrow 0, \tag{10}$$

where $B = -(1/2\pi)(\ln(k/2) + \gamma - i\pi/2)$ in 2D Helmholtz problem, $B = -(1/2\pi)(\ln(k/2) + \gamma)$ in 2D modified Helmholtz problem, $B = ik/4\pi$ in 3D Helmholtz problem, and $B = 0$ in 3D modified Helmholtz problem, $\gamma = 0.57721566490153286\ldots$. Therefore, we can get U^{jj} and Q^{jj} through U_0^{jj} and Q_0^{jj} with (9) and (10).

3. Numerical Results and Discussions

In this section, the efficiency, accuracy, and convergence of the SBM are tested to 2D and 3D Laplace, Helmholtz, and modified Helmholtz problems. The numerical accuracy is calculated by the relative root mean square errors (Rerr) Lerr(u) which is defined as follows:

$$\text{Lerr}\left(u\right) = \frac{\sqrt{(1/\text{TN})\sum_{k=1}^{\text{TN}}|u\left(k\right) - \overline{u}\left(k\right)|^2}}{\sqrt{(1/\text{TN})\sum_{k=1}^{\text{TN}}|\overline{u}\left(k\right)|^2}}, \tag{11}$$
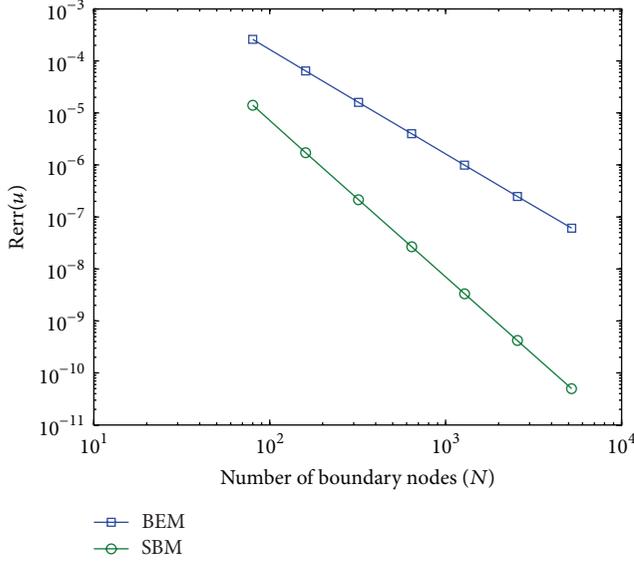
FIGURE 2: Relative errors of Example 1 by using the SBM and the BEM. $C_{\text{SBM}} = 3.0$; $C_{\text{BEM}} = 2.0$.

FIGURE 3: Condition numbers of the SBM and the BEM in Example 1.

where $\bar{u}(k)$ and $u(k)$ are the analytical and numerical solutions at x_i, respectively, and TN is the total number of test points in the interest domain. To demonstrate the convergence rate of the SBM and BEM, the following formulations are introduced:

$$C_{2D} = -\frac{\ln\left(\text{Error}\left(N_1\right)\right) - \ln\left(\text{Error}\left(N_2\right)\right)}{\ln\left(N_1\right) - \ln\left(N_2\right)}, \tag{12a}$$

$$\text{for 2D problems,}$$

$$C_{3D} = -2\frac{\ln\left(\text{Error}\left(N_1\right)\right) - \ln\left(\text{Error}\left(N_2\right)\right)}{\ln\left(N_1\right) - \ln\left(N_2\right)}, \tag{12b}$$

$$\text{for 3D problems,}$$

where Error(N_1) and Error(N_2) represent the errors Lerr(u) of the SBM and BEM with N_1 and N_2 boundary nodes, respectively. In the BEM, the direct formulation introduced in [1] is adopted and the integrations of the fundamental solution and its normal gradient over each element are calculated through 8-point Gauss quadrature for 2D problems and 9-point Gauss quadrature for 3D problems.

3.1. Error Analysis

3.1.1. 2D Laplace Problems

Example 1. Consider 2D Laplace problems in a circular domain with radius 1. And the exact solution is given by

$$u(x, y) = \cos(x)\exp(y). \tag{13}$$

Boundary conditions: all Dirichlet boundary conditions: $u(x_m) = \bar{u}(x_m)$, $x_m \in \Gamma_D$.

In this example, we use formula (6) to determine the SIFs. And the numerical results are shown in Figures 2 and 3.
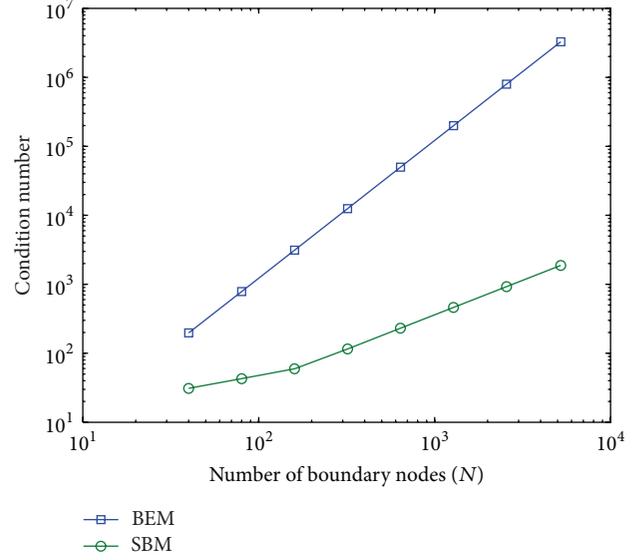
Example 2. Consider 2D Laplace problems in a square domain with length 1. And the exact solution is given by

$$u(x, y) = \cos(x)\exp(y). \tag{14}$$

Boundary conditions: $y = 0$ and $x = 1$ are Neumann boundary conditions; $\partial u(x_m)/\partial \mathbf{n} = \partial \bar{u}(x_m)/\partial \mathbf{n}$, $x_m \in \Gamma_N$. $x = 0$ and $y = 1$ are Dirichlet boundary conditions; $u(x_m) = \bar{u}(x_m)$, $x_m \in \Gamma_D$.

In this example, we use formulas (4) and (6) to determine the SIFs. The numerical results of SBM and BEM are shown in Figure 4.

3.1.2. 2D Helmholtz Problems

Example 3. Consider 2D Helmholtz problems in a circular domain with radius 1. And the exact solution is given by

$$u(x, y) = \cos(kx) + \cos(ky). \tag{15}$$

Boundary conditions: all Dirichlet boundary conditions: $u(x_m) = \bar{u}(x_m)$, $x_m \in \Gamma_D$.

In this example, we use formulas (6) and (9) to determine the SIFs. The numerical results of SBM and BEM when $k = 1$ are shown in Figure 5. Table 1 lists the numerical results of the SBM and the BEM with different wavenumbers ($k = 1$, $k = 10$, and $k = 20$).

Example 4. Consider 2D Helmholtz problems in a square domain with length 1. And the exact solution is given by

$$u(x, y) = \cos(kx) + \cos(ky). \tag{16}$$

Boundary conditions: $y = 0$ and $x = 1$ are Neumann boundary conditions; $\partial u(x_m)/\partial \mathbf{n} = \partial \bar{u}(x_m)/\partial \mathbf{n}$, $x_m \in \Gamma_N$. $x = 0$ and $y = 1$ are Dirichlet boundary conditions; $u(x_m) = \bar{u}(x_m)$, $x_m \in \Gamma_D$.

TABLE 1: Numerical results for Helmholtz problem in circular domain.

N	$k = 1$		$k = 10$		$k = 20$	
	SBM	BEM	SBM	BEM	SBM	BEM
40	$2.70E - 4$	$2.87E - 4$	$1.63E - 2$	$2.31E - 2$	$6.15E - 1$	$2.48E - 1$
80	$2.50E - 6$	$7.31E - 5$	$1.78E - 3$	$5.95E - 3$	$2.54E - 2$	$1.86E - 2$
160	$1.92E - 7$	$1.84E - 5$	$2.18E - 4$	$1.53E - 3$	$2.92E - 3$	$5.33E - 3$
320	$2.40E - 8$	$4.62E - 6$	$2.71E - 5$	$3.86E - 4$	$3.58E - 4$	$1.44E - 3$
640	$2.99E - 9$	$1.16E - 6$	$3.38E - 6$	$9.72E - 5$	$4.45E - 5$	$3.76E - 4$
1280	$3.74E - 10$	$2.89E - 7$	$4.23E - 7$	$2.43E - 5$	$5.56E - 6$	$9.59E - 5$
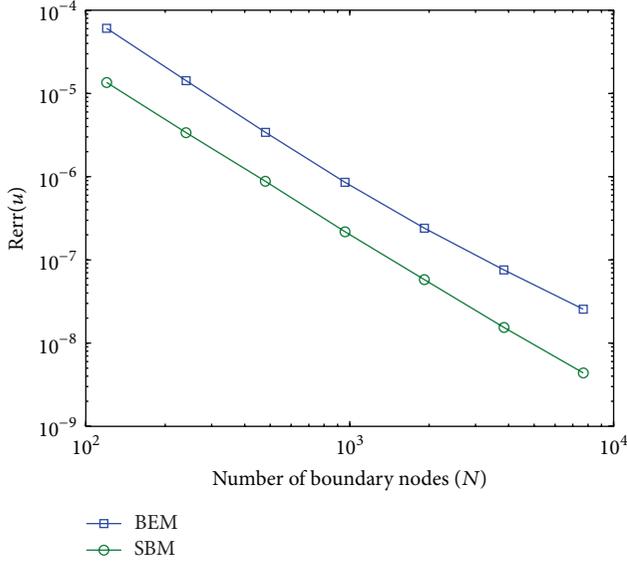
FIGURE 4: Relative errors of Example 2 by using the SBM and the BEM. $C_{\text{SBM}} = 1.9$; $C_{\text{BEM}} = 1.9$.
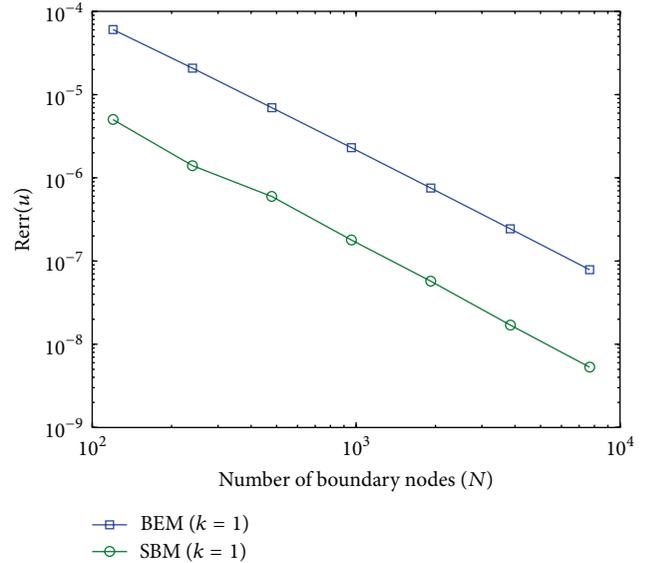
FIGURE 6: Relative errors of Example 4 by using the SBM and the BEM. $C_{\text{SBM}} = 1.6$; $C_{\text{BEM}} = 1.6$.

In this example, we use formulas (4), (6), (9), and (10) to determine the SIFs. The numerical results of SBM and BEM when $k = 1$ are shown in Figure 6.

3.1.3. 2D Modified Helmholtz Problems

Example 5. Consider 2D modified Helmholtz problems in a circular domain with radius 1. And the exact solution is given by

$$u(x, y) = \exp\left(k\frac{x + y}{\sqrt{2}}\right). \tag{17}$$

Boundary conditions: all Dirichlet boundary conditions: $u(x_m) = \overline{u}(x_m)$, $x_m \in \Gamma_D$.
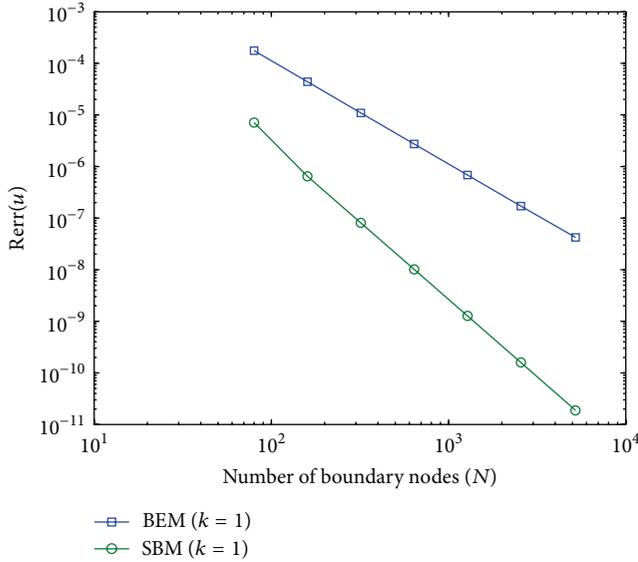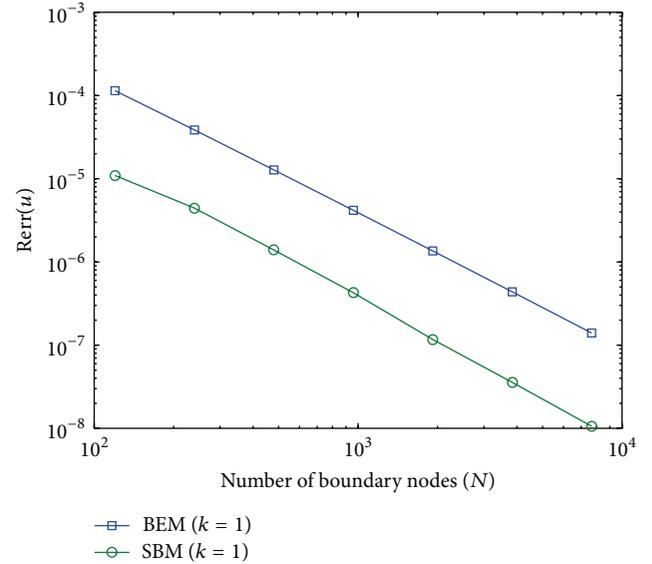
In this example, we use formulas (6) and (9) to determine the SIFs. The numerical results of SBM and BEM when $k = 1$ are shown in Figure 7.

Example 6. Consider 2D modified Helmholtz problems in a square domain with length 1. And the exact solution is given by

$$u(x, y) = \exp\left(k\frac{x + y}{\sqrt{2}}\right). \tag{18}$$

FIGURE 5: Relative errors of Example 3 by using the SBM and the BEM. $C_{\text{SBM}} = 3.1$; $C_{\text{BEM}} = 1.9$.

TABLE 2: Numerical results for Helmholtz problem in square domain.

N	$k = 1$		$k = 10$		$k = 20$	
	SBM	BEM	SBM	BEM	SBM	BEM
60	$4.51E - 3$	$3.31E - 4$	$5.01E - 2$	$6.81E - 3$	$1.33E - 1$	$2.51E - 2$
120	$1.10E - 5$	$1.14E - 5$	$1.27E - 4$	$2.28E - 3$	$9.99E - 4$	$7.71E - 3$
240	$4.44E - 6$	$3.86E - 5$	$3.99E - 5$	$7.28E - 4$	$1.93E - 4$	$2.28E - 3$
480	$1.39E - 6$	$1.28E - 5$	$1.10E - 5$	$2.30E - 4$	$3.70E - 5$	$6.90E - 4$
960	$4.27E - 7$	$4.18E - 6$	$3.40E - 6$	$7.24E - 5$	$9.00E - 6$	$2.06E - 4$
1920	$1.17E - 7$	$1.36E - 6$	$9.34E - 7$	$2.27E - 5$	$2.25E - 6$	$6.18E - 5$

BEM ($k = 1$)
SBM ($k = 1$)

FIGURE 7: Relative errors of Example 5 by using the SBM and the BEM. $C_{SBM} = 3.1$; $C_{BEM} = 2.0$.

BEM ($k = 1$)
SBM ($k = 1$)

FIGURE 8: Relative errors of Example 6 by using the SBM and the BEM. $C_{SBM} = 1.6$; $C_{BEM} = 1.6$.

Boundary conditions: $y = 0$ and $x = 1$ are Neumann boundary conditions; $\partial u(x_m)/\partial \mathbf{n} = \partial \overline{u}(x_m)/\partial \mathbf{n}$, $x_m \in \Gamma_N$. $x = 0$ and $y = 1$ are Dirichlet boundary conditions; $u(x_m) = \overline{u}(x_m)$, $x_m \in \Gamma_D$.

In this example, we use formulas (4), (6), (9), and (10) to determine the SIFs. The numerical results of SBM and BEM when $k = 1$ are shown in Figure 8. Table 2 lists the numerical results of the SBM and the BEM with different wavenumbers ($k = 1$, $k = 10$, and $k = 20$).

It can be observed that the present SBM performs more accurate solutions than the BEM with the same number of boundary nodes, and the SBM converge remarkably with the increasing boundary node number N. The error analysis shows that the present SBM have rapid convergence rate ($C_{2D} = 2$) in 2D problems. And, in some cases, the convergence rate can reach 3. In addition, the condition number of SBM is lower than BEM. Without mesh and integration, the SBM is computationally more efficient than the BEM.

3.1.4. 3D Laplace Problems

Example 7. Consider 3D Laplace problems in a sphere domain with radius 1. And the exact solution is given by

$$u(x, y, z) = \exp\left(\sqrt{2}z\right) \cos(x) \sin(y) + 1. \quad (19)$$

Boundary conditions: all Dirichlet boundary conditions: $u(x_m) = \overline{u}(x_m)$, $x_m \in \Gamma_D$.

In this example, we use formula (7) to determine the SIFs. The numerical results of SBM and BEM are shown in Figure 9.

Example 8. Consider 3D Laplace problems in a cube domain with length 1. And the exact solution is given by

$$u(x, y, z) = \exp\left(\sqrt{2}z\right) \cos(x) \sin(y) + 1. \quad (20)$$

Boundary conditions: $x = 1$, $y = 1$, and $z = 1$ are Neumann boundary conditions; $\partial u(x_m)/\partial \mathbf{n} = \partial \overline{u}(x_m)/\partial \mathbf{n}$, $x_m \in \Gamma_N$. $x = 0$, $y = 0$, and $z = 0$ are Dirichlet boundary conditions; $u(x_m) = \overline{u}(x_m)$, $x_m \in \Gamma_D$.

In this example, we use formulas (4) and (5) to determine the SIFs. The numerical results of SBM and BEM are shown in Figure 10.

Example 9. Consider 3D Laplace problems in a tire domain. The tire surface is defined by the following equation:

$$\{(x, y, z) \mid x = (R + r \cos \varphi) \cos \theta, \ y$$
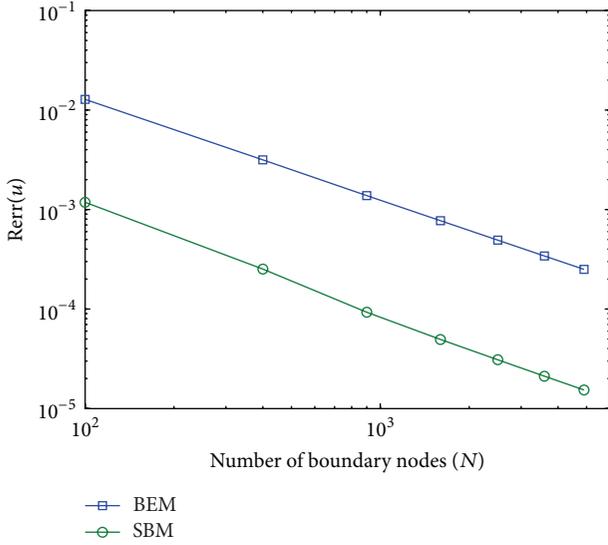$$= (R + r \cos \varphi) \sin \theta, \ z = r \sin \varphi, \ 0 \le \theta, \ \varphi < 2\pi\}, \quad (21)$$

FIGURE 9: Relative errors of Example 7 by using the SBM and the BEM. $C_{\text{SBM}} = 2.3$; $C_{\text{BEM}} = 2.0$.

FIGURE 10: Relative errors of Example 8 by using the SBM and the BEM. $C_{\text{SBM}} = 2.7$; $C_{\text{BEM}} = 2.6$.

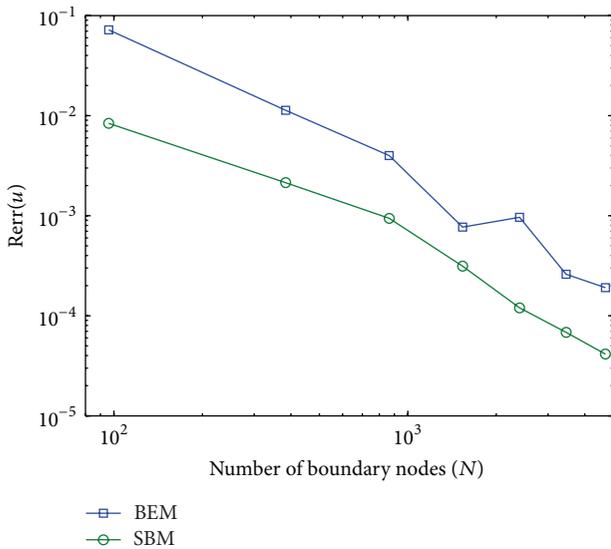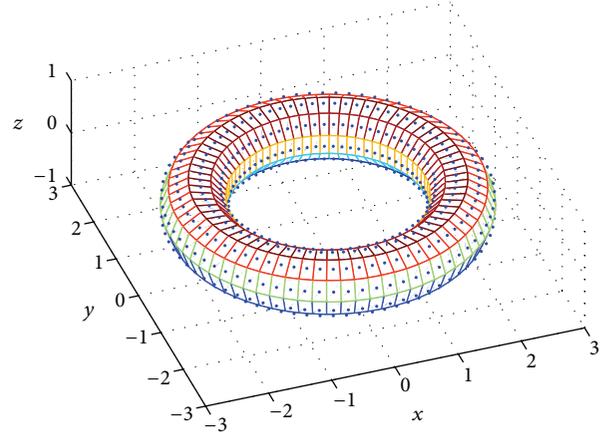FIGURE 11: The distribution of source points on tire surface.
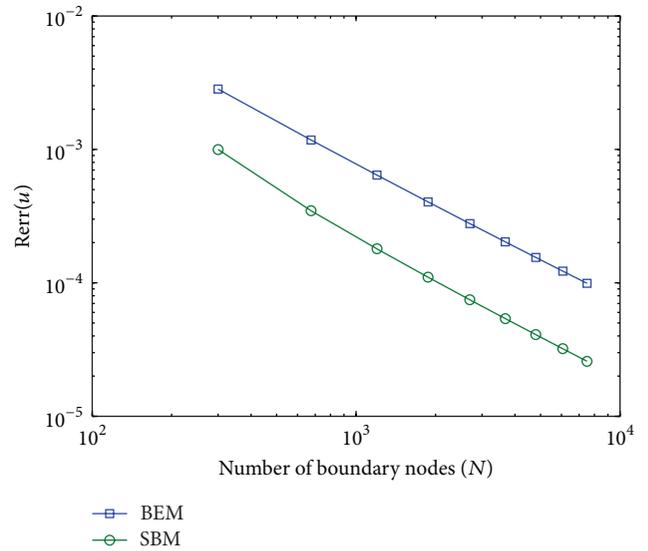
FIGURE 12: Relative errors of Example 9 by using the SBM and the BEM. $C_{\text{SBM}} = 2.3$; $C_{\text{BEM}} = 2.2$.

where $R = 2$, $r = 0.5$. The distribution of source points on tire surface is shown in Figure 11. And the exact solution is given by

$$u(x, y, z) = \exp\left(\sqrt{2}z\right)\cos(x)\sin(y) + 1. \qquad (22)$$

Boundary conditions: all Dirichlet boundary conditions: $u(x_m) = \overline{u}(x_m)$, $x_m \in \Gamma_D$.

In this example, we use formula (7) to determine the SIFs. The numerical results of SBM and BEM are shown in Figure 12.

3.1.5. 3D Helmholtz Problems

Example 10. Consider 3D Helmholtz problems in a sphere domain with radius 1. And the exact solution is given by

$$u(x, y, z) = \cos(kx) + \cos(ky) + \cos(kz). \qquad (23)$$

Boundary conditions:

(1) all Dirichlet boundary conditions: $u(x_m) = \overline{u}(x_m)$, $x_m \in \Gamma_D$.

(2) all Neumann boundary conditions: $\partial u(x_m)/\partial\mathbf{n} = \partial\overline{u}(x_m)/\partial\mathbf{n}$, $x_m \in \Gamma_N$.

In this example, we use formulas (7) and (9) to determine the SIFs in case (1) and formulas (4) and (10) to determine the SIFs in case (2). The numerical results of SBM and BEM when $k = 1$ are shown in Figures 13 and 14. Table 3 lists the numerical results of the SBM and the BEM in case (1) with different wavenumbers ($k = 1$, $k = 5$, and $k = 10$).

TABLE 3: Numerical results for Helmholtz problem in sphere domain in case (1).

N	k = 1		k = 5		k = 10	
	SBM	BEM	SBM	BEM	SBM	BEM
100	$1.51E-3$	$1.14E-2$	$1.74E-1$	$9.47E-2$	$8.09E-1$	$9.33E-1$
400	$3.84E-3$	$2.80E-3$	$2.70E-2$	$2.09E-2$	$1.27E-1$	$4.90E-2$
900	$1.58E-4$	$1.23E-3$	$9.66E-3$	$8.71E-3$	$3.16E-2$	$1.32E-2$
1600	$8.73E-5$	$6.94E-4$	$4.85E-3$	$4.79E-3$	$1.29E-2$	$7.42E-3$
2500	$5.53E-5$	$4.23E-4$	$2.90E-3$	$3.02E-3$	$6.57E-3$	$4.78E-3$

TABLE 4: Numerical results for Helmholtz problems in cube domain in case (2).

N	k = 1		k = 5		k = 10	
	SBM	BEM	SBM	BEM	SBM	BEM
96	$1.71E-3$	$5.11E-3$	$2.06E-2$	$1.03E-1$	$2.41E-1$	$1.83E-1$
384	$1.24E-4$	$1.59E-3$	$3.87E-3$	$3.81E-2$	$2.35E-2$	$3.19E-2$
864	$5.72E-5$	$9.03E-4$	$2.02E-3$	$1.90E-2$	$7.35E-3$	$1.44E-2$
1536	$2.70E-5$	$6.26E-4$	$1.48E-3$	$1.11E-2$	$3.38E-3$	$8.31E-3$
2400	$2.13E-5$	$4.78E-4$	$8.57E-4$	$7.08E-3$	$1.81E-3$	$5.37E-3$
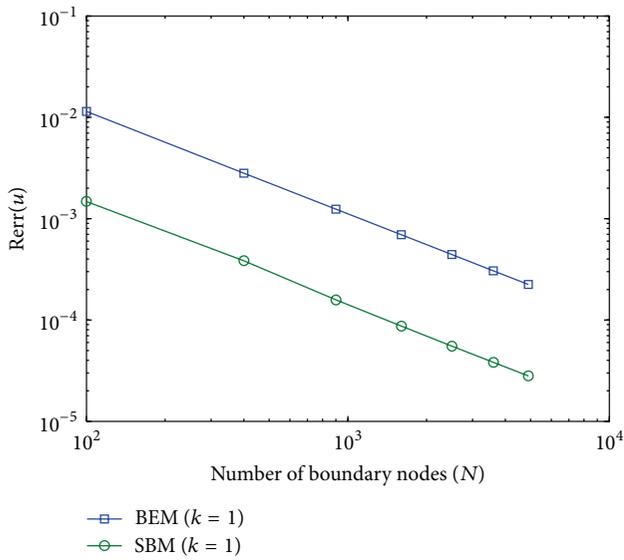
FIGURE 13: Relative errors of Example 10 when $k = 1$ by using the SBM and the BEM in case (1). $C_{SBM} = 2.1$; $C_{BEM} = 2.0$.
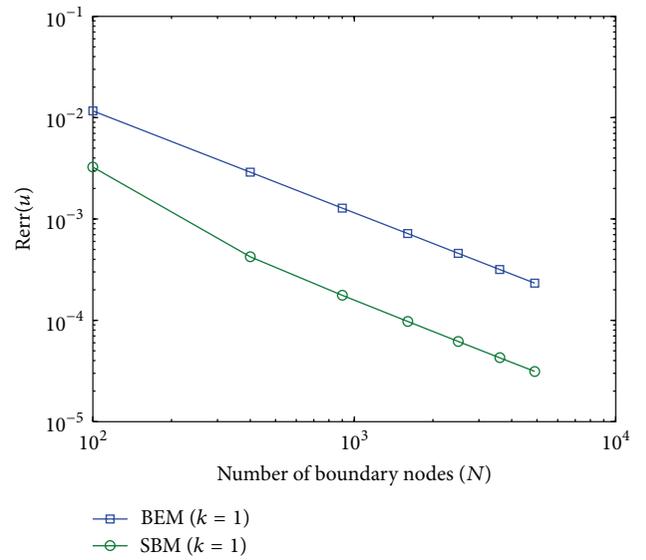
FIGURE 14: Relative errors of Example 10 when $k = 1$ by using the SBM and the BEM in case (2). $C_{SBM} = 2.1$; $C_{BEM} = 2.0$.

Example 11. Consider 3D Helmholtz problems in a cube domain with length 1 and the exact solution is given by

$$u(x, y, z) = \cos(kx) + \cos(ky) + \cos(kz). \qquad (24)$$

Boundary conditions:

(1) all Neumann boundary conditions: $\partial u(x_m)/\partial \mathbf{n} = \partial \overline{u}(x_m)/\partial \mathbf{n}, x_m \in \Gamma_N$.

(2) $x = 1$, $y = 1$, and $z = 1$ are Neumann boundary conditions; $\partial u(x_m)/\partial \mathbf{n} = \partial \overline{u}(x_m)/\partial \mathbf{n}$, $x_m \in \Gamma_N$. $x = 0$, $y = 0$, and $z = 0$ are Dirichlet boundary conditions; $u(x_m) = \overline{u}(x_m)$, $x_m \in \Gamma_D$.

In this example, we use formulas (4) and (10) to determine the SIFs in case (1) and formulas (4), (10), (5), and (9) to

determine the SIFs in case (2). The numerical results of SBM and BEM when $k = 1$ are shown in Figures 15–17. Table 4 lists the numerical results of the SBM and the BEM in case (2) with different wavenumbers ($k = 1$, $k = 5$, and $k = 10$).

Example 12. Consider 3D Helmholtz problems in a tire domain. The tire surface is defined by the following equation:

$$\{(x, y, z) \mid x = (R + r\cos\varphi)\cos\theta, \ x$$
$$= (R + r\cos\varphi)\sin\theta, \ y = r\sin\varphi, \ 0 \le \theta, \ \varphi < 2\pi\}, \qquad (25)$$

where $R = 2$, $r = 0.5$, and the exact solution is given by

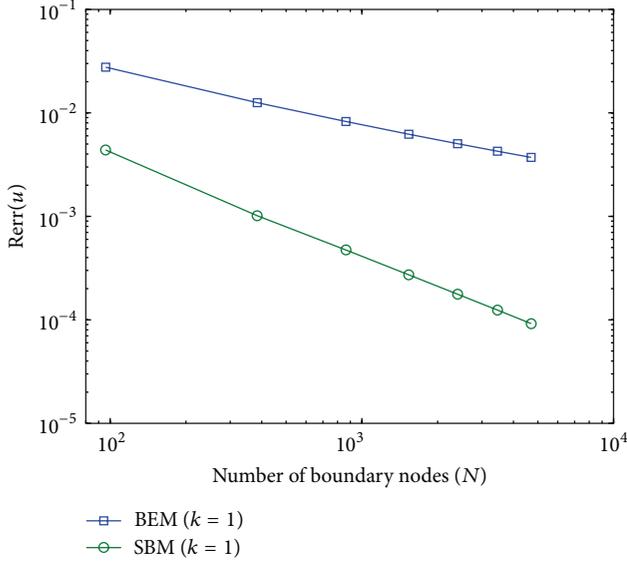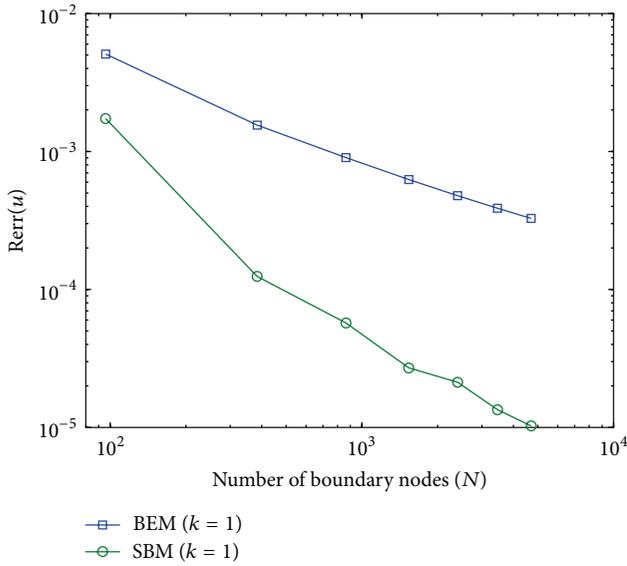$$u(x, y, z) = \cos(kx) + \cos(ky) + \cos(kz). \qquad (26)$$

FIGURE 15: Relative errors of Example 11 when k =1 by using the SBM and the BEM in case (1). $C_{\text{SBM}} = 2.0$; $C_{\text{BEM}} = 1.1$.
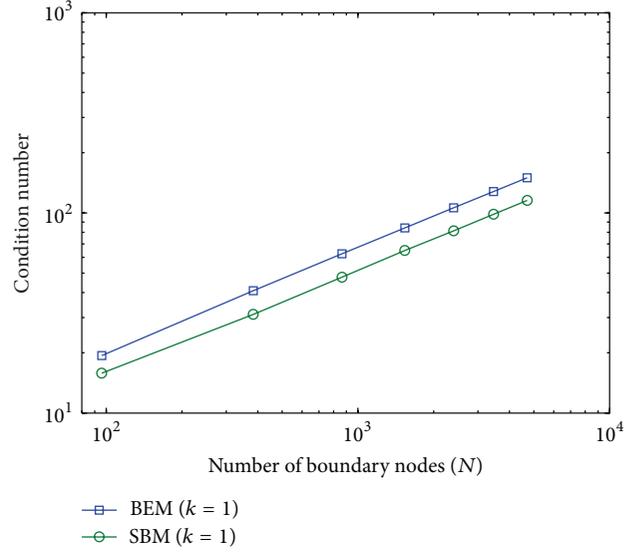

FIGURE 17: Condition numbers of Example 11 by using the SBM and the BEM in case (2).
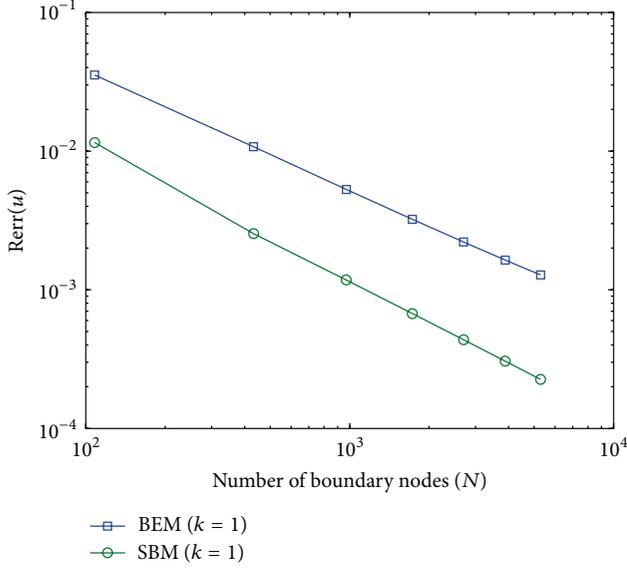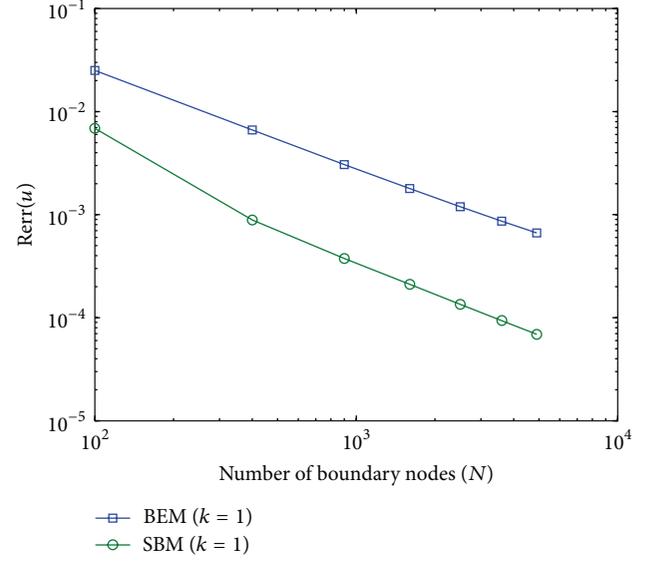

FIGURE 16: Relative errors of Example 11 when $k = 1$ by using the SBM and the BEM in case (2). $C_{\text{SBM}} = 2.3$; $C_{\text{BEM}} = 1.5$.
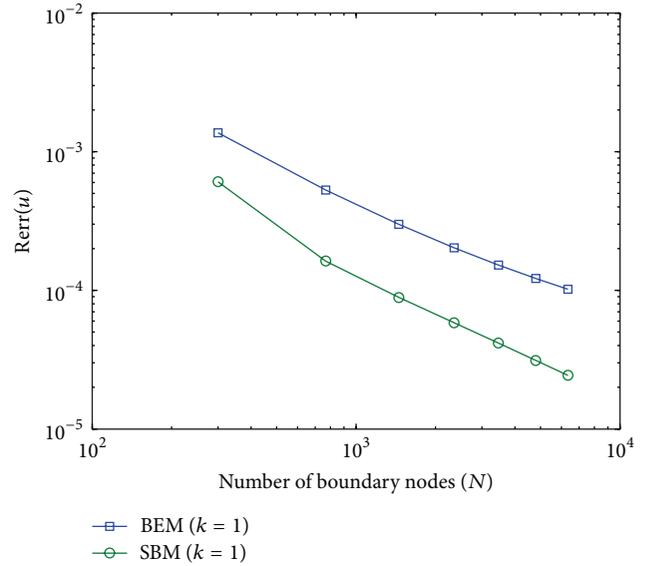
FIGURE 18: Relative errors of Example 12 when $k = 1$ by using the SBM and the BEM in case (1). $C_{\text{SBM}} = 1.9$; $C_{\text{BEM}} = 1.7$.

Boundary conditions:

    (1) all Dirichlet boundary conditions: $u(x_m) = \overline{u}(x_m)$, $x_m \in \Gamma_D$.

    (2) all Neumann boundary conditions: $\partial u(x_m)/\partial \mathbf{n} = \partial \overline{u}(x_m)/\partial \mathbf{n}$, $x_m \in \Gamma_N$.

In this example, we use formulas (7) and (9) to determine the SIFs in case (1) and formulas (4) and (10) to determine the SIFs in case (2). The numerical results of SBM and BEM when $k = 1$ are shown in Figures 18 and 19.

3.1.6. 3D Modified Helmholtz Problems

Example 13. Consider 3D modified Helmholtz problems in a sphere domain with radius 1. And the exact solution is given by

$$u(x, y, z) = \exp\left(k\frac{x + y + z}{\sqrt{3}}\right). \tag{27}$$

Boundary conditions:

    (1) all Dirichlet boundary conditions: $u(x_m) = \overline{u}(x_m)$, $x_m \in \Gamma_D$.

FIGURE 19: Relative errors of Example 12 when $k = 1$ by using the SBM and the BEM in case (2). $C_{SBM} = 2.0$; $C_{BEM} = 1.7$.

FIGURE 21: Relative errors of Example 13 when $k = 1$ by using the SBM and the BEM in case (2). $C_{SBM} = 2.2$; $C_{BEM} = 2.0$.
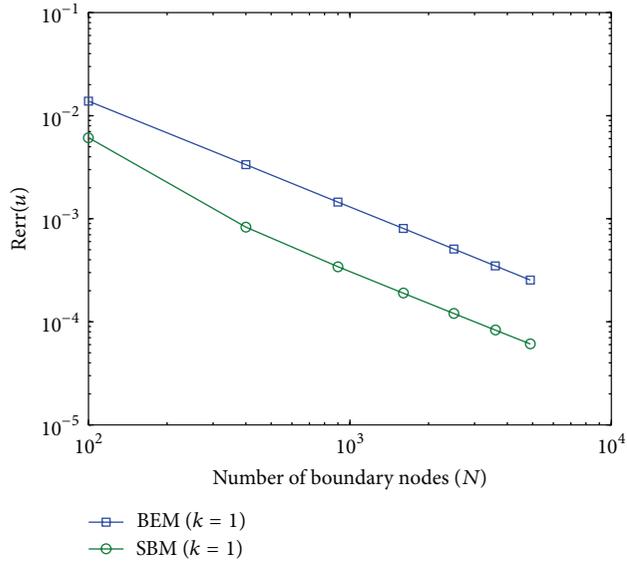

FIGURE 20: Relative errors of Example 13 when $k = 1$ by using the SBM and the BEM in case (1). $C_{SBM} = 2.1$; $C_{BEM} = 2.0$.
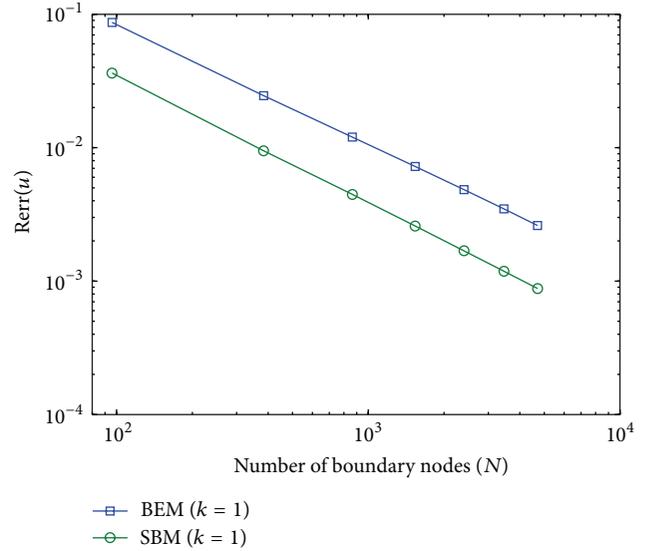

FIGURE 22: Relative errors of Example 14 when $k = 5$ by using the SBM and the BEM in case (1). $C_{SBM} = 1.9$; $C_{BEM} = 1.8$.

(2) all Neumann boundary conditions: $\partial u(x_m)/\partial \mathbf{n} = \partial \overline{u}(x_m)/\partial \mathbf{n}$, $x_m \in \Gamma_N$.

In this example, we use formulas (7) and (9) to determine the SIFs in case (1) and formulas (4) and (10) to determine the SIFs in case (2). The numerical results of SBM and BEM when $k = 1$ are shown in Figures 20 and 21.

Example 14. Consider 3D modified Helmholtz problems in a cube domain with length 1 and the exact solution is given by

$$u(x, y, z) = \exp\left(k\frac{x + y + z}{\sqrt{3}}\right). \tag{28}$$

Boundary conditions:

(1) all Neumann boundary conditions: $\partial u(x_m)/\partial \mathbf{n} = \partial \overline{u}(x_m)/\partial \mathbf{n}$, $x_m \in \Gamma_N$.

(2) $x = 1$, $y = 1$, and $z = 1$ are Neumann boundary conditions; $\partial u(x_m)/\partial \mathbf{n} = \partial \overline{u}(x_m)/\partial \mathbf{n}$, $x_m \in \Gamma_N$. $x = 0$, $y = 0$, and $z = 0$ are Dirichlet boundary conditions; $u(x_m) = \overline{u}(x_m)$, $x_m \in \Gamma_D$.

In this example, we use formulas (4) and (10) to determine the SIFs in case (1) and formulas (4), (10), (5), and (9) to determine the SIFs in case (2). The numerical results of SBM and BEM when $k = 5$ in case (1) and $k = 1$ in case (2) are shown in Figures 22 and 23. Table 5 lists the numerical

TABLE 5: Numerical results for modified Helmholtz problems in cube domain in case (1).

N	$k = 1$		$k = 5$		$k = 10$	
	SBM	BEM	SBM	BEM	SBM	BEM
96	$7.01E - 3$	$1.03E - 2$	$3.63E - 2$	$8.68E - 2$	$7.07E - 2$	$2.18E - 1$
384	$1.58E - 3$	$3.01E - 3$	$9.53E - 3$	$2.45E - 2$	$2.25E - 2$	$4.84E - 2$
864	$7.35E - 4$	$3.31E - 3$	$4.47E - 3$	$1.20E - 2$	$1.09E - 2$	$2.19E - 2$
1536	$4.25E - 4$	$3.29E - 3$	$2.61E - 3$	$7.21E - 3$	$6.41E - 3$	$1.29E - 2$
2400	$2.76E - 4$	$3.21E - 3$	$1.68E - 3$	$4.78E - 3$	$4.18E - 3$	$8.61E - 3$
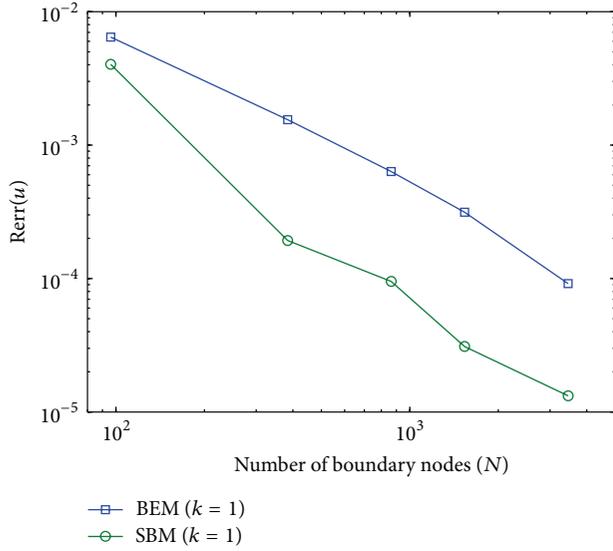
FIGURE 23: Relative errors of Example 14 when $k = 1$ by using the SBM and the BEM in case (2). $C_{\text{SBM}} = 2.4$; $C_{\text{BEM}} = 2.4$.

FIGURE 24: Relative errors of Example 15 when $k = 1$ by using the SBM and the BEM in case (1). $C_{\text{SBM}} = 3.1$; $C_{\text{BEM}} = 1.5$.

results of the SBM and the BEM in case (1) with different wavenumbers ($k = 1$, $k = 5$, and $k = 10$).

Example 15. Consider 3D modified Helmholtz problems in a tire domain. The tire surface is defined by the following equation:

$$\{(x, y, z) \mid x = (R + r \cos \varphi) \cos \theta, \; x$$
$$= (R + r \cos \varphi) \sin \theta, \; y = r \sin \varphi, \; 0 \leq \theta, \; \varphi < 2\pi\}, \quad (29)$$
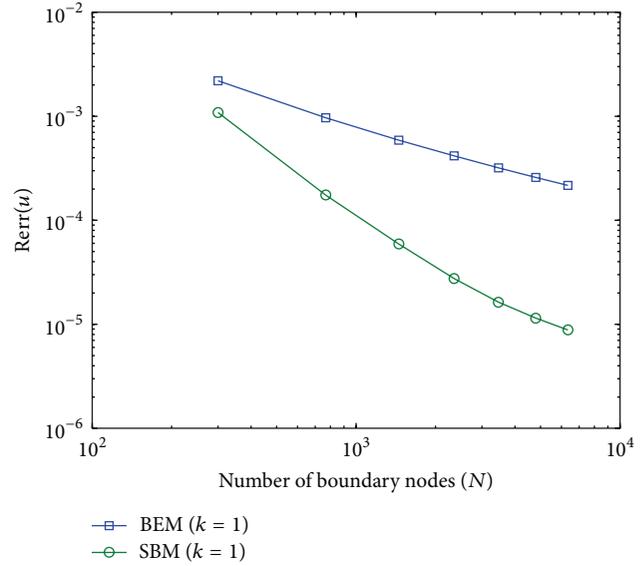
where $R = 2$, $r = 0.5$, and the exact solution is given by

$$u(x, y, z) = \exp\left(k \frac{x + y + z}{\sqrt{3}}\right). \quad (30)$$

Boundary conditions:

(1) all Dirichlet boundary conditions: $u(x_m) = \overline{u}(x_m)$, $x_m \in \Gamma_D$.

(2) all Neumann boundary conditions: $\partial u(x_m)/\partial \mathbf{n} = \partial \overline{u}(x_m)/\partial \mathbf{n}$, $x_m \in \Gamma_N$.

In this example, we use formulas (7) and (9) to determine the SIFs in case (1) and formulas (4) and (10) to determine the SIFs in case (2). The numerical results of SBM and BEM when $k = 1$ are shown in Figures 24 and 25.

It can be observed that the present SBM performs more accurate solutions than the BEM with the same number of boundary nodes, and the SBM converge remarkably with the increasing boundary node number N. The error analysis shows that the present SBM have rapid convergence rate ($C_{\text{3D}} = 2$) in all these 3D examples.

4. Conclusion

This short communication makes an extensive investigation on numerical efficiency and convergence rates of the SBM to several 2D and 3D benchmark examples about Laplace, Helmholtz, and modified Helmholtz equations in comparison with the direct BEM.

Through numerical experiments, we find that the present SBM results are in good agreement with the exact solutions in both 2D and 3D problems. And the SBM converge remarkably with the increasing boundary node number N. The error analysis shows that the present SBM have rapid convergence rate ($C_{\text{2D}} = C_{\text{3D}} = 2$) in both 2D and 3D problems for Laplace, Helmholtz, and modified Helmholtz equations. And, in some cases, the convergence rate of SBM can reach 3. In addition, we find from the tables that the present SBM results are still in good agreement with the exact
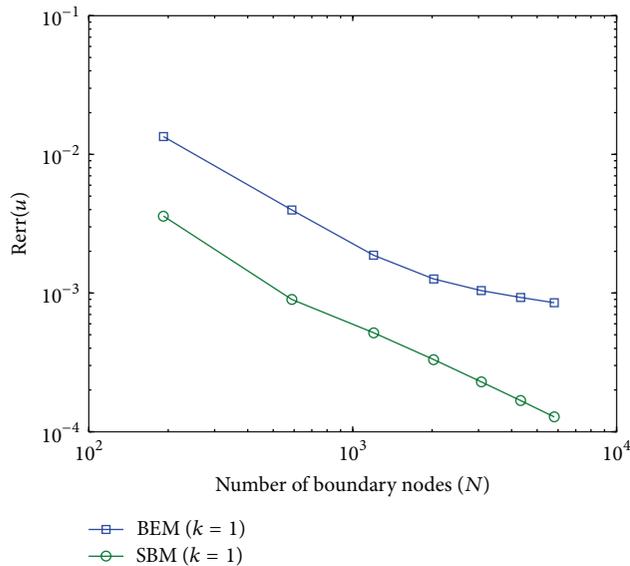
FIGURE 25: Relative errors of Example 15 when $k = 1$ by using the SBM and the BEM in case (2). $C_{\text{SBM}} = 2.0$; $C_{\text{BEM}} = 1.5$.

solutions in Helmholtz and modified Helmholtz problems with different wavenumber.

Furthermore, we find that in most cases the SBM and BEM have similar convergence rates, while the SBM has slightly better accuracy than the direct BEM. In addition, the condition number of SBM is lower than BEM in most cases. Without mesh and integration, the SBM is computationally more efficient than the BEM.

Competing Interests
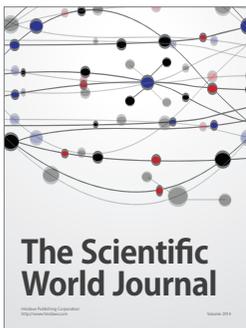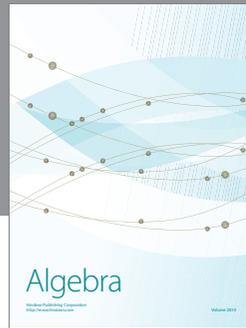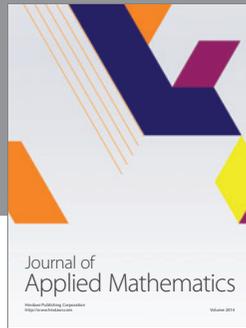
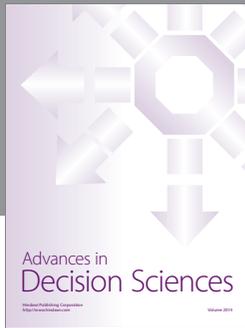The authors declare that they have no competing interests.

Acknowledgments

References

[1] P. K. Banerjee, *The Boundary Element Methods in Engineering*, Mcgraw-Hill Book Company, London, UK, 1994.

[2] J. T. Chen, K. H. Chen, I. L. Chen, and L. W. Liu, "A new concept of modal participation factor for numerical instability in the dual BEM for exterior acoustics," *Mechanics Research Communications*, vol. 30, no. 2, pp. 161–174, 2003.

[3] A. H.-D. Cheng and D. T. Cheng, "Heritage and early history of the boundary element method," *Engineering Analysis with Boundary Elements*, vol. 29, no. 3, pp. 268–302, 2005.

[4] M. Cui, W.-z. Feng, X.-w. Gao, and K. Yang, "High order projection plane method for evaluation of supersingular curved boundary integrals in BEM," *Mathematical Problems in Engineering*, vol. 2016, Article ID 9523405, 8 pages, 2016.

[5] G. Fairweather and A. Karageorghis, "The method of fundamental solutions for elliptic boundary value problems," *Advances in Computational Mathematics*, vol. 9, no. 1-2, pp. 69–95, 1998.

[6] C. S. Chen, C. M. Fan, and J. Monroe, "The method of fundamental solutions for solving elliptic partial differential equations with variable coefficients," in *The Method of Fundamental Solutions—A Meshless Method*, C. S. Chen, A. Karageorghis, and Y. S. Smyrlis, Eds., pp. 75–105, Dynamic Publishers, Atlanta, Ga, USA, 2008.

[7] J. R. Berger and A. Karageorghis, "The method of fundamental solutions for heat conduction in layered materials," *International Journal for Numerical Methods in Engineering*, vol. 45, no. 11, pp. 1681–1694, 1999.

[8] C. S. Chen, A. Karageorghis, and Y. S. Smyrlis, *The Method of Fundamental Solutions-A Meshless Method*, Dynamic Publishers, Atlanta, Ga, USA, 2008.

[9] J. T. Chen, M. H. Chang, K. H. Chen, and I. L. Chen, "Boundary collocation method for acoustic eigenanalysis of three-dimensional cavities using radial basis function," *Computational Mechanics*, vol. 29, no. 4-5, pp. 392–408, 2002.

[10] C.-S. Liu, "A highly accurate MCTM for inverse Cauchy problems of Laplace equation in arbitrary plane domains," *Computer Modeling in Engineering and Sciences*, vol. 35, no. 2, pp. 91–111, 2008.

[11] C.-M. Fan, H.-F. Chan, C.-L. Kuo, and W. Yeih, "Numerical solutions of boundary detection problems using modified collocation Trefftz method and exponentially convergent scalar homotopy algorithm," *Engineering Analysis with Boundary Elements*, vol. 36, no. 1, pp. 2–8, 2012.

[12] C.-C. Tsai and P.-H. Lin, "A multiple-precision study on the modified collocation trefftz method," *Computers, Materials & Continua*, vol. 28, no. 3, pp. 231–259, 2012.

[13] D. L. Young, K. H. Chen, and C. W. Lee, "Novel meshless method for solving the potential problems with arbitrary domain," *Journal of Computational Physics*, vol. 209, no. 1, pp. 290–321, 2005.

[14] D. L. Young, K. H. Chen, and C. W. Lee, "Singular meshless method using double layer potentials for exterior acoustics," *Journal of the Acoustical Society of America*, vol. 119, no. 1, pp. 96–107, 2006.

[15] D. L. Young, K. H. Chen, T. Y. Liu, L. H. Shen, and C. S. Wu, "Hypersingular meshless method for solving 3D potential problems with arbitrary domain," *Computer Modeling in Engineering and Sciences*, vol. 40, no. 3, pp. 225–269, 2009.

[16] K.-H. Chen, M.-C. Lu, and H.-M. Hsu, "Regularized meshless method analysis of the problem of obliquely incident water wave," *Engineering Analysis with Boundary Elements*, vol. 35, no. 3, pp. 355–362, 2011.

[17] B. Šarler, "Solution of potential flow problems by the modified method of fundamental solutions: formulations with the single layer and the double layer fundamental solutions," *Engineering Analysis with Boundary Elements*, vol. 33, no. 12, pp. 1374–1382, 2009.

[18] M. Perne, B. Šarler, and F. Gabrovšek, "Calculating transport of water from a conduit to the porous matrix by boundary distributed source method," *Engineering Analysis with Boundary Elements*, vol. 36, no. 11, pp. 1649–1659, 2012.

[19] S. Kim, "An improved boundary distributed source method for two-dimensional Laplace equations," *Engineering Analysis with Boundary Elements*, vol. 37, no. 7-8, pp. 997–1003, 2013.

[20] A. K. Khambampati, Y.-G. Lee, K. Y. Kim, D. W. Jerng, and S. Kim, "A meshless improved boundary distributed source method for two-phase flow monitoring using electrical resistance tomography," *Engineering Analysis with Boundary Elements*, vol. 52, pp. 1–15, 2015.

[21] E. Sincich and B. Šarler, "Non-singular method of fundamental solutions based on Laplace decomposition for 2D stokes flow problems," *Computer Modeling in Engineering & Sciences*, vol. 99, no. 5, pp. 393–415, 2014.

[22] W. Chen, "Singular boundary method: a novel, simple, mesh-free, boundary collocation numerical method," *Chinese Journal of Solid Mechanics*, vol. 30, no. 6, pp. 592–599, 2009.

[23] Z.-J. Fu, W. Chen, and Y. Gu, "Burton-Miller-type singular boundary method for acoustic radiation and scattering," *Journal of Sound and Vibration*, vol. 333, no. 16, pp. 3776–3793, 2014.

[24] L. L. Sun, W. Chen, and A. H. D. Cheng, "Singular boundary method for 2D dynamic poroelastic problems," *Wave Motion*, vol. 61, pp. 40–62, 2016.

[25] W. Z. Qu, W. Chen, and Y. Gu, "Fast multipole accelerated singular boundary method for the 3D Helmholtz equation in low frequency regime," *Computers & Mathematics with Applications*, vol. 70, no. 4, pp. 679–690, 2015.

[26] J. P. Li, Z. J. Fu, and W. Chen, "Numerical investigation on the obliquely incident water wave passing through the submerged breakwater by singular boundary method," *Computers Mathematics with Applications*, vol. 71, no. 1, pp. 381–390, 2016.